Clinical Testing of an Optimized Software Solution for an Automated, Observer-Independent Evaluation of Dopamine Transporter SPECT Studies

Walter Koch, MD[1]; Perry E. Radau, PhD[2]; Christine Hamann, MD[3]; and Klaus Tatsch, MD[1]

[1]Department of Nuclear Medicine, University of Munich, Munich, Germany; [2]Department of Medical Biophysics, Sunnybrook & Women's College Health Sciences, Toronto, Ontario, Canada; and [3]Department of Neurology, University of Munich, Munich, Germany

A lack of standardized evaluation procedures for dopamine transporter (DAT) SPECT investigations impairs both intra- and interindividual comparisons as well as multicenter trials—for example, for assessment of disease progression or the response to various drug treatments. Therefore, the aim of this study was to evaluate a novel automated method, which has been specifically developed for a standardized quantification of *N*-(3-fluoropropyl)-2β-carbomethoxy-3β-(4-iodophenyl)nortropane (^{123}I-FP-CIT) SPECT studies. **Methods:** DAT binding ratios of 155 ^{123}I-FP-CIT SPECT studies in 14 control subjects and 141 patients referred to confirm or exclude a presynaptic dopaminergic deficit were determined manually and by a fully automated technique. The latter included coregistration of patient studies to an ^{123}I-FP-CIT mean template of controls with specialized, nonrigid adjustment for variation in striatal location, followed by calculation of specific striatal DAT binding using a standardized 3-dimensional volume-of-interest (VOI) map. The map is based on a MR scan and covers the striatum (S), caudate (C), putamen (P), and an occipital reference region. The semiquantitative ratios of both methods were compared with the visual findings. **Results:** Excellent linear correlations were observed between manually and automatically determined results (S: $r = 0.99$; C: $r = 0.99$; P: $r = 0.99$; $P < 0.001$, respectively). Automated evaluations delivered highly reproducible and visually exact coregistrations. Individual variations in striatal anatomy (e.g., atrophy) were considered and VOI positions were corrected before quantification. Both the manual and the automated method showed identical accuracy in supporting the visual diagnoses. **Conclusion:** In a large patient population, excellent agreement was observed between quantitative DAT results using a time-consuming, observer-dependent, conventional manual method and the objective, automated evaluation specifically developed for a standardized evaluation of ^{123}I-FP-CIT SPECT studies. It is suggested that the novel automated technique may substantially facilitate both intra- and interindividual comparisons as well as multicenter trials.

Key Words: quantitative evaluation; FP-CIT; automatic data processing; dopamine transporter

J Nucl Med 2005; 46:1109–1118

Imaging of the dopaminergic system with SPECT has become widespread in Europe, since ligands for imaging the presynaptic dopamine transporter (DAT) (e.g., *N*-(3-fluoropropyl)-2β-carbomethoxy-3β-(4-iodophenyl)nortropane [^{123}I-FP-CIT]) as well as dopamine D_2 receptors (e.g., iodobenzamide [^{123}I-IBZM]) are commercially available. ^{123}I-FP-CIT is a valuable tool for discriminating neurodegenerative parkinsonian syndromes with an associated presynaptic dopaminergic deficit from diseases without presynaptic neurodegeneration (e.g., essential tremor) (*1*). Besides visual assessment of SPECT images, semiquantitative evaluation of the radiotracer binding plays an important role in interpreting the results. Accurate semiquantification allows comparison of a single patient scan with normal reference values and enables follow-up investigations to monitor disease progression and therapeutic effects. For this purpose, a variety of manual, operator-intensive techniques have been developed. Unfortunately, inter- and intraobserver variability arises in manual methods and may hamper the reproducibility and accuracy of results. Manual techniques not only require precise realignment of the studies resulting in a standardized slice orientation but also depend on drawing and placement of regions of interest (ROIs). Since this is a time-consuming process, most manual quantification approaches either use only a few single or added slices out of the entire SPECT reconstruction volume for quantification.

Although techniques for the anatomic standardization of perfusion SPECT studies or metabolic PET data to standard

Received Jan. 26, 2005; revision accepted Mar. 29, 3005.

For correspondence contact: Dr. med. Walter Koch, Department of Nuclear Medicine, University of Munich, Marchioninistrasse 15, 81377 Munich, Germany.

E-mail: walter.koch@med.uni-muenchen.de

brain templates are well established (*2–5*), fully automated investigation of presynaptic DAT studies is challenging. Compared with perfusion studies, SPECT ligands such as ^{123}I-FP-CIT show high specific binding only in areas with a high density of the specific neurons addressed with this tracer. Therefore, resulting images contain considerably fewer anatomic details. This not only impairs the success rate of single-step automatic registration algorithms available on many imaging workstations but also limits the use of manual landmark registration techniques (*6*). Considerable variability in the exact location of the striatum, mostly caused by atrophy or ventricle enlargement, can cause additional difficulties.

This article presents clinical results obtained with an automated software solution specifically developed for the processing of DAT SPECT studies.

MATERIALS AND METHODS

Subjects

Fourteen healthy control subjects free of neurologic diseases (age range, 39–74 y; mean ± SD, 57 ± 11 y) and 141 consecutive patients (age range, 23–85 y; mean ± SD, 61 ± 11 y) with findings suggestive of parkinsonian syndromes were included in this retrospective data analysis. The patients were referred for ^{123}I-FP-CIT SPECT to establish or exclude the diagnosis of parkinsonian syndromes. Thus, a broad spectrum ranging from normal findings to severely decreased DAT binding was included. Both healthy control subjects and patients gave informed consent.

SPECT

Data were acquired with a triple-head γ-camera (Picker Prism 3000) using low-energy, high-resolution fanbeam collimators. Acquisition was started exactly 4 h after intravenous injection of 185 MBq of the commercially available radiopharmaceutical ^{123}I-FP-CIT (Amersham Health, part of GE Healthcare). A 128 × 128 matrix was used for all acquisitions. The rotational radius was minimized and was <13 cm in all cases. One hundred twenty projections were acquired at 60 s per view with the camera heads following a circular orbit, resulting in a total scan time of 43 min. Total brain counts of >2 million were achieved in all examinations. The projection data were checked visually for patient motion using the cine display and sinograms provided by the software of the camera manufacturer (Odyssey-FX software; Philips). Studies with excessive patient motion were discarded.

SPECT data were reconstructed by filtered backprojection, filtered with a Butterworth 3-dimensional (3D) postfilter (0.60 cycle/cm, fifth order) and corrected for attenuation according to Chang's method (μ = 0.11/cm, elliptic fitting with separate contours for each slice).

Automated Evaluation Method

The automated semiquantification software is based on a modified version of the Brain Analysis Software (BRASS, version 3.4.4; Hermes Medical Solutions) running on a Hermes workstation (Nuclear Diagnostics). It is based on a multistep registration of individual patient studies to a template of healthy controls and subsequent application and fine adjustment of a standardized 3D volume-of-interest (VOI) map to measure semiquantitative values. Mean counts per voxel values for each VOI as well as ratios of the entire striatum, the caudate nucleus, and the putamen to the occipital cortex are calculated. For this software approach, the template and the 3D VOI map had to be created.

Creation of Template of Healthy Control Subjects and Corresponding VOI Map. The SPECT template (Fig. 1) was created specifically for ^{123}I-FP-CIT SPECT scans using the images of healthy controls. This template provides mean values for each voxel. The template was created in several steps:

First, a MRI scan of a single healthy control subject was aligned manually according to the Talairach coordinates. Next, 14 SPECT studies of the healthy volunteers were coregistered to that MR scan and the accuracy of the registration was assessed visually. Then a

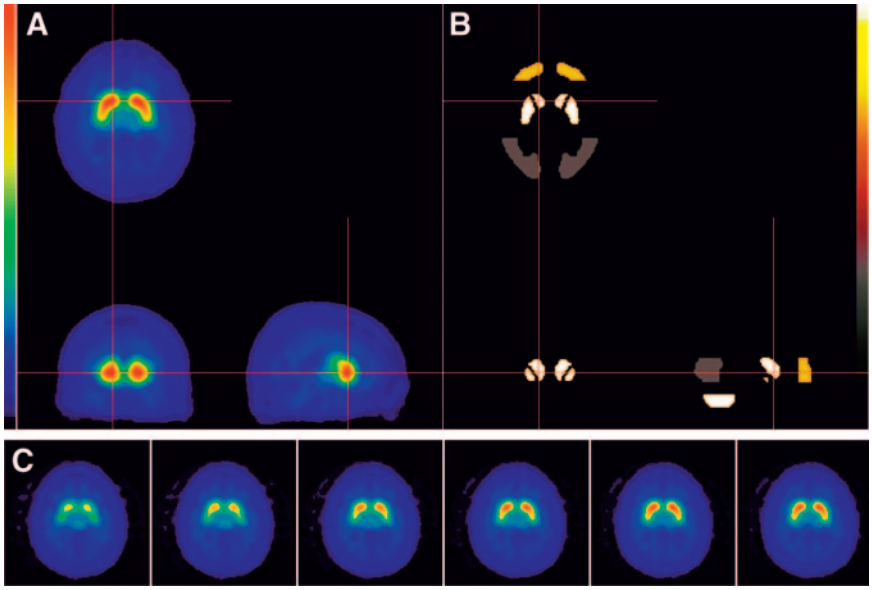

FIGURE 1. Mean template of healthy control subjects (A and C) and corresponding 3D VOI map (B) for semiquantitative evaluation.

standardized 3D, bilateral symmetric VOI map (Fig. 1) was generated based on the MRI scan with separate regions covering the entire striatum (1,409 voxels), the caudate (524 voxels), the putamen (689 voxels), as well as 3 different reference areas: frontal cortex (2,982 voxels), occipital cortex (8,537 voxels), and cerebellum (3,614 voxels).

With the VOI map defined, all 14 SPECT studies were normalized by the counts in the occipital reference region and the set of means calculated formed an initial template. To further increase the template accuracy, the registration of all 14 healthy control subjects was repeated with the preliminary template serving as reference study for the registration. The result of this process is the final normal template for use in the BRASS software. The voxel dimensions of the template were 2.0 × 2.0 × 2.0 mm.

Registration Process. Individual patient studies were then registered to the ^{123}I-FP-CIT template by applying an automated fitting algorithm, including an adjustment of the VOI map to adjust the striatal VOIs separately for each hemisphere to compensate for individual anatomic variation (e.g., atrophy).

The registration method uses 3 separate registration steps. In the first step, the individual study is registered to the mean template, adjusting 9 parameters (3 each for rotation, translation, and anisotropic scaling) of an alignment transformation matrix, using the principal axes technique and an iterative, simplex algorithm to maximize normalized mutual information, a measure of similarity between the transformed individual study and the template (*7–9*).

The second and third steps provide a fine adjustment (6-parameter translation and rotation) of the striatal VOIs separately for each hemisphere to adjust for individual anatomic differences. This is accomplished by masking the opposite hemisphere, applying a 30% threshold to the template to minimize the influence of extrastriatal regions, followed by fitting the patient image to the template image. The result is that the patient image will be matched to the VOI map for the calculation of intensity in the striatum of one hemisphere. The third step repeats the procedure for the opposite hemisphere. The fine-adjustment transforms have no effect on the calculation of reference VOI intensities.

Assessment of Accuracy of Automatic Registration. To describe the accuracy of the automated registration of an individual patient study to the template, the study alignment was visually evaluated. Both the accuracy of the brain surface registration as well as the positioning of the VOIs were rated. For this purpose, the major type of error was classified into one of the categories: anterior–posterior shift, lateral shift, inferior–superior shift, transverse angle, sagittal angle, coronal angle, brain too large compared with template, and brain too small compared with template. Next, the extent of the misalignment was recorded in pixels (for deviation of VOIs and brain size compared with template, where 1 pixel = 2 mm) or in degrees (for angulation errors). Classification and estimation of the extent of the major type of error were recorded separately for the striatal area and the occipital reference region. For further analyses, the categories were combined into errors of VOI shift (anterior–posterior, lateral shift, inferior–superior shift), study rotation (transverse, sagittal, coronal) or study scaling (brain too large or too small compared with the template).

Whether manual correction of the VOI positioning was required or whether the automated alignment was sufficiently accurate was decided on the extent of the major type of error from a clinician's point of view. Circumstances under which the alignment was manually corrected are defined in Table 1.

Reproducibility and Observer Independence of Automatic Technique. To estimate the reproducibility of the automated semiquantification under different initial orientation conditions, original images were misaligned before automated analysis. Twelve randomly generated misalignments were tested in a subset of 20 randomly selected scans, resulting in a total of 240 registrations. Each misalignment affected all 6 parameters for shift and rotation (maximum extent arbitrarily confined to ±5 pixel shift, ±10° rotation in transverse and coronal angle, ±15° rotation in sagittal angle). The reproducibility of the quantification was defined as the SD of the specific striatal binding ratio across misalignment trials as done previously in a work by Radau et al. (*10*). Left and right striatum were included as separate datasets into the analyses. The striatal binding ratios of the 20 subjects included showed a gaussian distribution with a mean ± SD of 1.7 ± 0.7. Since no user interference was required in the 240 registrations, the inter- and intraobserver variability was completely eliminated.

Manual Evaluation Method

To validate the automated technique, each study was also analyzed using a semiquantitative manual evaluation method established in our institution for routine clinical interpretation of ^{123}I-FP-CIT studies. For that purpose, the reconstructed transverse slices of each scan were first visually aligned parallel to the orbitomeatal line. The 4 slices containing the image count maximum within the striatal area were summed to form a single slice (resulting in a slice thickness of 9 mm with 2.27 × 2.27 mm pixel

TABLE 1
Circumstances Under Which Manual Correction of Automated VOI Positioning Was Considered Necessary from a Clinician's Point of View and Number of Scans Affected

Conditions	*n*
For manual correction of striatal VOI positioning	
Shift of single basal ganglia VOI of >2 mm	0/155
Brain too small compared with template with both basal ganglia VOIs being >4 mm too far apart (in most cases, resulting in shift of >2 mm on each side)	2/155
Rotational misalignment of >3° in any plane	0/155
For manual correction of occipital reference VOI positioning	
VOI shift resulting in overlap of any part of occipital reference region with either skull or ventricles of >4 mm	6/155
Rotational misalignment of >3° in any plane resulting in overlap of reference VOI with either skull or ventricles	1/155

dimensions). A standardized, symmetric set of predefined 2-dimensional (2D) ROIs for the striatum (91 pixels), caudate (32 pixels), and putamen (38 pixels) was loaded, and each ROI was manually adjusted (affecting shift and rotation, but without changes of the ROI size) to match the corresponding structures (Fig. 2). In addition, a freehand ROI was drawn, which covers the occipital cortex and serves as reference region (size variable, ~300 pixels).

Comparison Between Manual and Automated Method

Comparison of Semiquantitative Results Between Both Methods. The semiquantitative results of both evaluation techniques were compared. For this purpose, the specific radiotracer binding ratios of striatum, caudate, and putamen were calculated with the occipital cortex serving as the reference region (specific $\text{binding}_{\text{striatum}}$ = [striatum – occipital reference]/occipital reference). Since the underlying disease in patients with parkinsonian syndromes often affects the caudate nucleus and putamen with different severity, the putamen-to-caudate ratio (ratio between the specific binding in the putamen and the caudate) was also calculated for both methods of analyses.

Visual Interpretation. All 155 scans were read by a specialist in the field of DAT imaging who was unaware of the referring diagnoses and the semiquantitative evaluation. On the basis of the pattern of radiotracer uptake in the striatum, the decision between normal (sickle-shaped uptake in both caudate and putamen) and neurodegenerative parkinsonian syndrome (reduced uptake predominantly in the putamen or strong asymmetry) was made (*11*).

Time Required for Processing Individual Studies. To estimate the time required to analyze an individual patient study using both the manual and the automatic evaluation approaches, the time needed to entirely process a subset of 10 randomly selected patients using both methods was recorded. For the automated method, both the processing time on the computer system (batch run on a Hermes workstation with a 1.8-GHz Pentium 4 processor and 512-MB RAM) and the time required by an experienced physician to check the registration and transfer the quantification results to a database were recorded. For the manual method, the time needed to realign the studies, place the ROIs, and enter the quantification results in the database as well as documentation by an experienced physician was recorded.

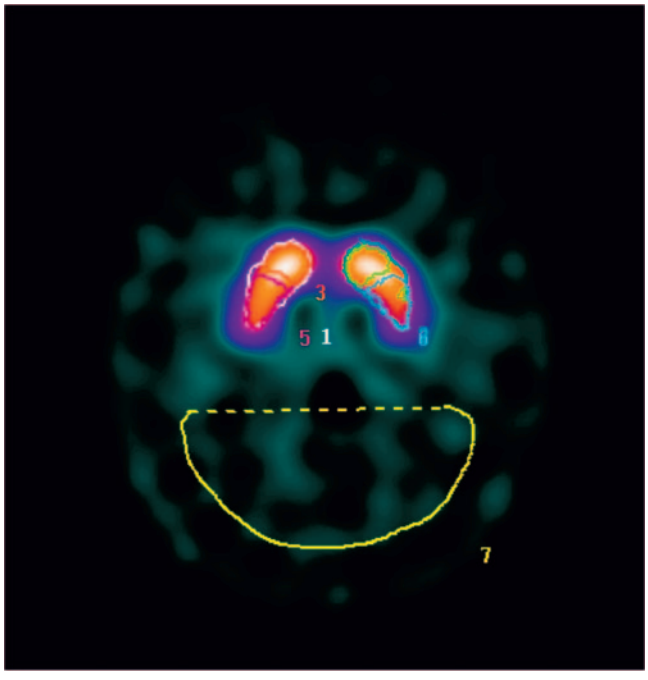

FIGURE 2. Example for manual semiquantification technique. Predefined 2D ROIs are placed manually to match entire striatum, caudate, and putamen (regions 1–6). In addition, a freehand ROI is drawn as occipital reference (region 7).

Statistics

Correlations between semiquantitative results evaluated by the automated method and the manual method were calculated using linear regression analyses. For regression statistics as well as linear regression analyses, the right and the left striatal regions were included as separate datasets. Simple correlation coefficients only provide limited insight into the agreement between 2 methods of analysis. To further estimate the range of deviations expected when replacing the manual method by the automated method, the difference between the semiquantitative ratios of both methods averaged over all scans ($\bar{d}$), the corresponding SD (s) as well as the limits of agreement ($\bar{d} - 2s$ and $\bar{d} + 2s$) were calculated as proposed by Bland and Altman (*12*). In addition, a variation index was defined according to Verhoeff et al. (*13*) and Seibyl et al. (*14*) as used for test/retest variation testing in these studies:

$$\text{Variation index (\%)} = \frac{\text{abs(automated ratio} - \text{manual ratio)} \cdot 200\%}{\text{automated ratio} + \text{manual ratio}},$$

where abs stands for absolute value.

Since the binding ratios evaluated by the automated method were lower than those of the manual method (shown by a linear regression slope lower than that of the line of equality), the semiquantitative values evaluated using the automated method had to be corrected first to be directly comparable to the manual approach and to calculate the statistics. For this purpose, all binding ratios were multiplied with the reciprocal slope of the regression curve. These values are further referred to as "corrected" semiquantitative ratios.

The diagnostic accuracy of the manual and the automated evaluation in comparison with the visual findings was measured by the area under the curve (AUC) of receiver-operating-characteristic (ROC) analyses. Furthermore, the reference value of 2.7 established in our Department of Nuclear Medicine (based on previous scans of healthy control subjects) to differentiate between normal and pathologic specific striatal binding was applied to the mean of left and right striatal binding results of both the manual and the automated method (using corrected values) for each scan. Comparisons between the resulting classification of the manual approach, the automated method, and the visual uptake pattern were performed using cross tables. Cohen's κ and McNemar P values were calculated.

All statistical analyses have been performed using SPSS software (SPSS Inc.).

TABLE 2
Main Reasons for Suboptimal Automated VOI Positioning

Reasons	*n* or %
For suboptimal positioning of striatal VOIs	50/155
Suboptimal scaling of patient study compared with template/3D VOIs	52%
Imprecise rotation of patient study compared with template/3D VOIs	32%
Misplacement (shift) of 3D VOIs	16%
For suboptimal positioning of reference VOIs	26/155
Suboptimal scaling of patient study	42%
Imprecise rotation or shift of patient study	58%

RESULTS

Automatic Registration

By visual assessment, automated fitting of the patient studies to the template and placement of VOIs was successful in the majority of all cases (sufficiently accurate placement of basal ganglia VOIs in 153/155 cases and of the reference region in 148/155 cases) with need for a manual adjustment according to the conditions defined in Table 1 in only 9 of 155 scans. In the latter cases, the placement was adjusted manually and the quantification results were included, as it would have been recommended in a clinical setting. In several scans, VOI placement only slightly fails to match the optimal position, not requiring correction. Table 2 summarizes the dominating reasons for suboptimal fitting, independent of the extent of the misalignment and with inclusion of barely noticeable misplacement of the VOIs in any direction. All 14 studies of healthy control subjects were fitted accurately.

Figure 3 exemplarily shows a patient scan adequately registered to the template with the VOIs correctly placed and a scan with inadequate registration and VOI placement.

The average SD of the striatal binding ratios as a measure for the reproducibility of the semiquantification process, tested with a series of 12 misalignments for 20 scans, was 0.05 ± 0.02.

Comparison with Established Manual Approach

The correlations between automated and manually evaluated DAT (^{123}I-FP-CIT) studies are summarized in Figure 4 and Table 3, where specific binding ratios for the right and the left hemispheric regions were included as separate datasets. There were no systematic differences in the correlation between the results obtained in healthy control subjects and those of patient scans. Specific ratios calculated using the automated evaluation were lower than those of the manual evaluation. After correcting for this finding, the mean differences of the specific binding ratios between the manual and automated approach are given in Table 4, with the corresponding limits of agreement and the variation indices.

Comparison of Semiquantitative Results with Visual Interpretation

The AUC of the ROC analyses comparing the specific binding ratios with the visual finding of neurodegeneration versus normal uptake pattern was identical for the manual and the automated evaluation in the striatal (0.97), the caudate (0.92), and the putaminal region (0.99). Applying a previously established discrimination reference value of 2.7 for specific striatal binding to distinguish between patients with and without presynaptic deficit led to a classification consistent with the visual diagnosis in 141 of 155 cases for the automated method and in 142 of 155 cases for the manual method. One hundred forty-six of 155 scans were classified identically by both semiquantification methods (Cohen's $\kappa = 0.84$; McNemar $P = 0.18$). Most of the remaining 9 cases with contrary results between visual and semiquantitative analyses had striatal binding ratios close to the reference value. The corresponding visual diagnosis was matched correctly in 5 of 9 of these scans by the manual evaluation and in 4 of 9 cases by the automated evaluation. In 7 studies, neither semiquantitative method matched the visual findings.

Comparison of Processing Times

The mean processing time for the automated registration and VOI placement (averaged among the subset of 10

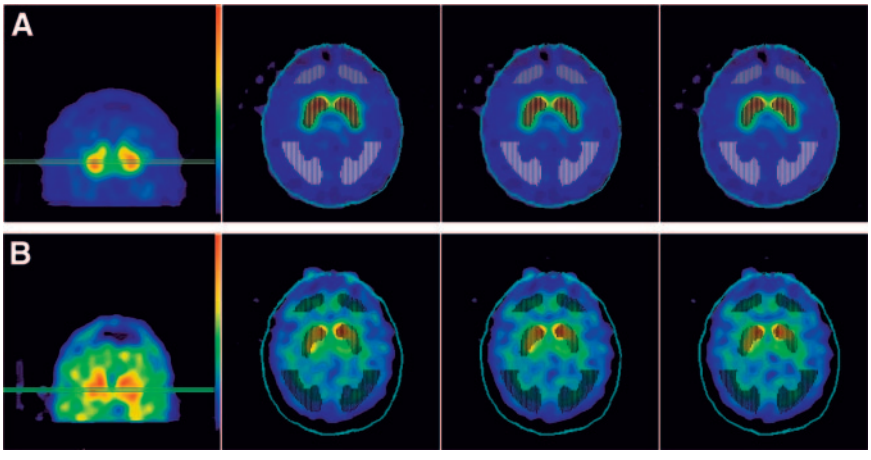

FIGURE 3. Example of a patient scan adequately registered to template with VOIs placed correctly (A) and a scan with inadequate registration (insufficient scaling) and imprecise VOI placement requiring manual correction (B). White line marks surface of the patient head of registration template used.

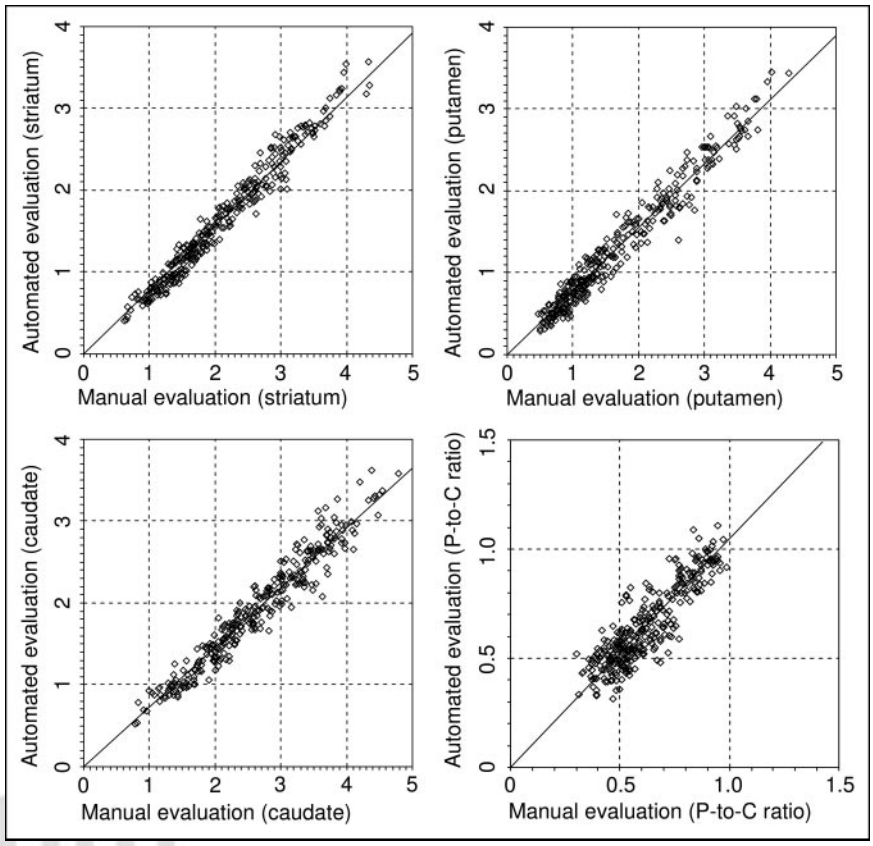

FIGURE 4. Correlation graphs of specific binding ratios obtained with manual and automatic semiquantification method ($P < 0.001$ in all 4 diagrams; 155 subjects, left and right striatum of all subjects included as separate data points). Corresponding regression line parameters are listed in Table 3. P-to-C ratio = putamen-to-caudate ratio.

patient studies) was 2 min 53 s per study. After the automated registration, the physician had to check the alignment, create prints, and transfer the results to our database, which required an additional 60 s.

For the manual semiquantitation, a mean time of 10 min 2 s per study was required (including reorientation, ROI placement, as well as printing and database entry).

DISCUSSION

Imaging of the presynaptic DAT has evolved into an important diagnostic tool for patients with parkinsonian syndromes (*15–18*) and, thus, has become a routine clinical procedure in nuclear medicine departments across Europe. In many cases, visual assessment of DAT SPECT studies enables clinicians to decide whether neurodegeneration of presynaptic neurons has occurred and to confirm or exclude a neurodegenerative parkinsonian syndrome (*19*). Especially for early diagnosis, the detection of subtle changes in DAT binding in striatal subregions, and for monitoring disease progression (*20–22*) or the beneficial effects of putative neuroprotective drugs, additional semiquantitative measurements are mandatory (*11*).

TABLE 3
Parameters of Linear Regression Line Between Manual and Automated Evaluations of Specific Binding Ratios

Specific binding	Striatum	Caudate	Putamen	P-to-C ratio
Healthy controls ($n = 14$)				
R^2	1.00	0.99	1.00	0.99
Slope ± SE	0.81 ± 0.01	0.74 ± 0.01	0.80 ± 0.01	1.07 ± 0.01
Patients ($n = 141$)				
R^2	1.00	1.00	0.99	0.98
Slope ± SE	0.78 ± 0.00	0.73 ± 0.00	0.77 ± 0.00	1.04 ± 0.01
Total ($n = 155$)				
R^2	0.99	0.99	0.99	0.98
Slope ± SE	0.79 ± 0.00	0.73 ± 0.00	0.78 ± 0.01	1.05 ± 0.01

P-to-C ratio = putamen-to-caudate ratio.
All correlations were statistically significant with $P < 0.001$.

TABLE 4
Deviation Between Semiquantitative Measures of Manual and Automated Method

Parameter	Striatum	Caudate	Putamen	P-to-C ratio
Mean difference ± SD	0.03 ± 0.17	0.02 ± 0.23	0.03 ± 0.19	0.06 ± 0.09
Limits of agreement	−0.37 to 0.30	−0.47 to 0.43	−0.41 to 0.36	−0.12 to 0.24
Variation index ± SD (%)	7.6 ± 6.2	7.1 ± 5.7	11.7 ± 9.2	13.8 ± 10.0

P-to-C ratio = putamen-to-caudate ratio.

Heretofore, manual ROI analyses have been used for semiquantification in many departments. Assuming optimal standardization of this technique, the interobserver variation in data processing can be minimized (*23*) but surely not entirely ruled out. In work by Verhoeff et al., considerable observer dependence was found when imaging the dopamine D_2 receptors with ^{123}I-IBZM (*13*).

Therefore, observer-independent automated systems are required to standardize the semiquantification process and to overcome observer dependency. The literature has addressed this problem in the past for various neurologic tracers. The first step of an automated study processing is usually a registration process of an individual patient study to a template of healthy control subjects. This can either be the general template provided by the statistical parametric mapping (SPM) software package (derived from ^{15}O PET studies) or a tracer-specific template (*4*). After successful registration, both voxelwise comparisons (cluster growing) and VOI analyses are available to analyze the resulting images. Voxel-based methods are well established (*24*), but VOI analyses are less susceptible to registration errors (*25*). In this context, for example, a study by Radau et al. on analyses of dopamine D_2 receptor imaging (*10*) showed that VOI analyses are more suitable for clinical routine and voxelwise comparisons did not achieve better diagnostic accuracy in discriminating idiopathic versus nonidiopathic parkinsonian syndromes.

On the basis of these facts, an "ideal" algorithm for an automated observer-independent evaluation of ^{123}I-FP-CIT studies should allow one to register the individual patient study to a tracer-specific template of healthy control subjects and then to apply a standardized 3D VOI map for semiquantification. The BRASS software is able to perform these tasks, and previous studies have shown its superiority compared with SPM in other brain applications such as perfusion SPECT (*5*). Furthermore, the software has proven to be reliable, reproducible, and easy to use in routine work (*5,7,10,26*).

For an accurate registration of studies to a template, the known features of parkinsonian syndromes must be considered. A major problem is that a strict linear fit of individual studies to a template often does not sufficiently compensate for anatomic variations of the basal ganglia location, especially in patients with cerebral atrophy. In other brain imaging, such as FDG PET, warp fitting has been applied to compensate for individual variation. Unfortunately, in progressive stages of parkinsonian syndromes there is little residual activity found in the caudate nucleus and almost none in the putaminal area, which might result in incorrect transformation (e.g., the caudate being deformed to match to the size of the entire striatum), introducing new sources of error. Techniques using simultaneously acquired transmission CT data as an intermediate dataset for coregistration, as established by Van Laere et al. (*27*), will also not provide sufficient information to adjust for intersubject differences in striatal size, angulation, and location due to the low soft-tissue contrast. Here, the additional morphologic correlation might only help to adjust the overall brain size but the transmission scan adds more dose and window contamination to the scan than desirable. Due to the specific demands related to DAT SPECT, the BRASS software had to be further modified and optimized. For this purpose, we implemented a multistep linear registration algorithm that not only registers the individual patient study to a mean template of healthy control subjects but also provides fine adjustment of the 3D VOIs to compensate for individual anatomic variation without requiring additional transmission CT data.

Automated fitting of the patient studies to the template and placement of the VOI map were successful in the majority of all cases without a need for manual adjustment. The algorithm showed excellent compensation for individual anatomic conditions (e.g., atrophy). Relevant misplacement occurred only in a few cases (~6%) and was mainly observed in patients with a relatively small brain size compared with the template, most probably due to a scaling limit of ±10% implemented in the current software version. In these patients, the striatal regions were occasionally placed too far lateral in both hemispheres and occipital ROIs exceeded the brain's outer surface. Originally, these scaling limits were implemented to prevent errors in cases where brain size was difficult to calculate from the low-intensity background. Consequently, future improvements might be obtained by modifying and optimizing the scaling estimate.

The 3D VOI map used in the automated method covers the entire striatum and was relatively stable concerning

misalignment. In contrast, various manual semiquantification techniques consider only a few transverse slices for analysis (*11*), so that small reorientation errors can cause significant asymmetry. An excellent correlation was observed between the manual and automatic evaluation for the VOI covering the entire striatum, whereas the correlation in the smallest striatal subregion (caudate) showed a slightly higher variability, even if the R^2 values were comparable. Smaller regions tend to be more sensitive to misalignment (in both the manual and the automatic approach) and this also explains the marginally higher variability. Another aspect to consider is that the algorithm adjusts only the VOI covering the entire striatum to match the individual patient study and assumes a fixed anatomic relation between caudate and putamen within the striatum. This might explain the slightly lower R^2 values for the putamen-to-caudate ratio. Therefore, if one considers this ratio as a predictor for an early parkinsonian syndrome, special attention must be paid to the accuracy of the VOI positioning. The algorithm does not currently compensate for individual rotational deviation of the basal ganglia shape, which—even though rare—has been shown to be the second most frequent reason for automated VOI misplacement.

The specific ratios calculated using the BRASS software were lower than those of the manual evaluation, similar to what has been described for the use of BRASS in imaging the dopamine D_2 receptor before (*10*). Since there is no evidence for regional variation of the DAT distribution within the striatum in autoradiographic studies (*28*), this effect can most probably be attributed to the larger number of pixels comprised in the 3D VOIs. These cover the entire striatum (with lower average counts per voxel) in comparison with only 4 slices with the highest intensity used by the 2D regions of the manual approach. An additional influence of counts in the reference region is rather unlikely, since both the standardized and freehand-drawn occipital regions are relatively large compared with the basal ganglia regions and, hence, less influenced by partial-volume effects. A slightly different relation of the number of pixels in the caudate, the putaminal, and the striatal VOI between the manual and the automated method most likely explains why the regression slopes show slightly different values for the caudate (0.73), the putamen (0.78), and the entire striatum (0.79). After correcting the specific binding ratios of the automated evaluation for the different regression slopes, the automated approach delivered striatal binding ratios in the range of 0.4 lower than to 0.3 higher than those measured using the manual method. Since the literature reports considerably larger differences in specific binding between patients with and without neurodegeneration (average DAT binding loss of 57% in the putamen, as reported by Tissingh et al. (*29*)), the observed range of differences of both evaluation methods will unlikely lower the diagnostic power. In addition, the variation index of the semiquantitative measures of bothmethods (8%) is not higher than the variability range of repeated scans observed in test/retest studies (*14,30–33*). Much of this variation between the manual and the automated techniques can likely be explained by the inherent intra- and interoperator variability of the manual technique, whereas the automated method delivers observer-independent results. This is also supported by findings of Linke et al. (*23*), who used the identical manual method for semiquantification of striatal ^{123}I-IPT binding and have shown an interobserver variability (9.1% ± 10.7%) and intraobserver variability (4.9% ± 5.3%) comparable with the variation indices found in our study. Even the higher variability in the putamen in the study by Linke et al. (interobserver, 12.0% ± 14.2%; intraobserver, 7.2% ± 6.9%) was found in a similar proportion in our data.

The ability of both the manual and the automated method to discriminate between patients with and without neurodegeneration of the presynaptic neuron is even more important than quantitative agreement of both approaches. However, a proven diagnosis can only be obtained by postmortem studies. Whereas movement disorder specialists can reach an accuracy of >90% in clinical diagnosis, general practitioners misdiagnose parkinsonism in up to a quarter of the cases (*34–36*). Because not all patients in our study have been seen by a movement disorder specialist and no reliable clinical long-term follow-up and no pathologic data are available for all of our patients, we compared the semiquantitative striatal binding ratios of both the manual approach and the automated method with the visual pattern of radiotracer uptake. This is particularly important in a clinical setting, since semiquantitative values are intended to represent the visual uptake pattern objectively and to assist less-experienced readers in determining the correct diagnoses. Both the identical high AUC of the ROC analysis and the high agreement of scan classification as normal or abnormal (based on the specific striatal binding and an established reference value) suggest equal clinical performance of both semiquantification methods. In 7 cases, however, both semiquantification approaches failed to match the visual finding when considering absolute specific striatal binding ratios. In one patient, this was due to the patient's age, since our reference value is not corrected for the normal loss of DAT binding with aging (*37,38*). In the other 6 patients, a prominent asymmetry of semiquantitative ratios indicated a pathologic result but the absolute binding ratios were still normal.

The assessment of reproducibility using randomly misaligned scans demonstrated that the automated fitting was very robust and the misalignments had only small effects on the binding ratios.

Summarizing, despite minor inaccuracies in automated alignments, the automated method provided very robust results for routine evaluation of ^{123}I-FP-CIT SPECT scans.

The automated evaluation of studies using the modified BRASS software is less time-consuming than the manual method previously used in our department. The calculation

of the registration parameters and the positioning of the VOIs require the majority of time but can be executed unattended through batch processing. The automated transfer of the quantification results to a database and to the medical report, as established in our department, minimizes the clinical reporting time.

CONCLUSION

The introduced software is a valuable tool in clinical routine evaluations of ^{123}I-FP-CIT SPECT scans of the DAT. The method provides objective and observer-independent semiquantification of the ligand binding in the striatum using a standardized 3D VOI map that covers the entire striatal volume. The reproducible quantification results showed an excellent correlation with manual semiquantification methods and identical accuracy in supporting the visual diagnoses. Automated processing is, in addition, less time-consuming than manual reorientation and ROI placement.

Currently, semiquantitative results calculated by the BRASS software are still specific for the camera system used (including type of camera, collimator, acquisition, and reconstruction parameters) and, hence, reference values of healthy control subjects cannot easily be transferred to other equipment. Since a recent study by Meyer et al. (*39*) shows an almost linear correlation of the ratios obtained with 2 different types of cameras, additional phantom measurements with anthropomorphic phantoms might allow the calculation of correction factors to correct between different camera equipment. This could make the software an indispensable objective tool for between-center comparisons and for use in multicenter trials.

The expandability of the automated processing algorithms to other tracers raises opportunities for extending this method. The creation of an IBZM mean template in a preliminary study also enabled use of the identical 3D VOI map for the comparative assessment of pre- and postsynaptic data in a single patient (*40*).

ACKNOWLEDGMENT

Financial support was received from Nuclear Diagnostics (Sweden).

REFERENCES

1. Pirker W, Asenbaum S, Bencsits G, et al. [^{123}I]Beta-CIT SPECT in multiple system atrophy, progressive supranuclear palsy, and corticobasal degeneration. *Mov Disord.* 2000;15:1158–1167.
2. Eberl S, Kanno I, Fulton RR, Ryan A, Hutton BF, Fulham MJ. Automated interstudy image registration technique for SPECT and PET. *J Nucl Med.* 1996;37:137–145.
3. Chang DJ, Zubal IG, Gottschalk C, et al. Comparison of statistical parametric mapping and SPECT difference imaging in patients with temporal lobe epilepsy. *Epilepsia.* 2002;43:68–74.
4. Gispert JD, Pascau J, Reig S, et al. Influence of the normalization template on the outcome of statistical parametric mapping of PET scans. *Neuroimage.* 2003;19:601–612.
5. Van Laere KJ, Warwick J, Versijpt J, et al. Analysis of clinical brain SPECT data based on anatomic standardization and reference to normal data: an ROC-based comparison of visual, semiquantitative, and voxel-based methods. *J Nucl Med.* 2002;43:458–469.
6. Sipila O, Nikkinen P, Pohjonen H, et al. Accuracy of a registration procedure for brain SPET and MRI: phantom and simulation studies. *Nucl Med Commun.* 1997;18:517–526.
7. Radau PE, Slomka PJ, Julin P, Svensson L, Wahlund LO. Evaluation of linear registration algorithms for brain SPECT and the errors due to hypoperfusion lesions. *Med Phys.* 2001;28:1660–1668.
8. Hill DL, Maurer CR Jr, Studholme C, Fitzpatrick JM, Hawkes DJ. Correcting scaling errors in tomographic images using a nine degree of freedom registration algorithm. *J Comput Assist Tomogr.* 1998;22:317–323.
9. Studholme C, Hawkes DJ, Hill DL. A normalized entropy measure for multimodality image alignment. In: Hansen KM, ed. *Proceedings of SPIE: Medical Imaging 1998—Image Processing.* Bellingham, WA: SPIE; 1998:132–143.
10. Radau PE, Linke R, Slomka PJ, Tatsch K. Optimization of automated quantification of ^{123}I-IBZM uptake in the striatum applied to parkinsonism. *J Nucl Med.* 2000;41:220–227.
11. Tatsch K, Asenbaum S, Bartenstein P, et al. European Association of Nuclear Medicine procedure guidelines for brain neurotransmission SPET using ^{123}I-labelled dopamine D_2 transporter ligands. *Eur J Nucl Med Mol Imaging.* 2002;29:BP30–BP35.
12. Bland JM, Altman DG. Statistical methods for assessing agreement between two methods of clinical measurement. *Lancet.* 1986;1:307–310.
13. Verhoeff NP, Kapucu O, Sokole-Busemann E, van Royen EA, Janssen AG. Estimation of dopamine D2 receptor binding potential in the striatum with iodine-123-IBZM SPECT: technical and interobserver variability. *J Nucl Med.* 1993;34:2076–2084.
14. Seibyl JP, Marek K, Sheff K, et al. Test/retest reproducibility of iodine-123-betaCIT SPECT brain measurement of dopamine transporters in Parkinson's patients. *J Nucl Med.* 1997;38:1453–1459.
15. Booij J, Speelman JD, Horstink MW, Wolters EC. The clinical benefit of imaging striatal dopamine transporters with [^{123}I]FP-CIT SPET in differentiating patients with presynaptic parkinsonism from those with other forms of parkinsonism. *Eur J Nucl Med.* 2001;28:266–272.
16. Oertel WH, Gerstner A, Hoffken H, Dodel RC, Eggert KM, Moller JC. Role of dopamine transporter SPECT for the practitioner and the general neurologist. *Mov Disord.* 2003;18(suppl 7):S9–S15.
17. Poewe W, Scherfler C. Role of dopamine transporter imaging in investigation of parkinsonian syndromes in routine clinical practice. *Mov Disord.* 2003;18(suppl 7):S16–S21.
18. Marshall V, Grosset DG. Role of dopamine transporter imaging in the diagnosis of atypical tremor disorders. *Mov Disord.* 2003;18(suppl 7):S22–S27.
19. Benamer TS, Patterson J, Grosset DG, et al. Accurate differentiation of parkinsonism and essential tremor using visual assessment of [^{123}I]-FP-CIT SPECT imaging: The [^{123}I]-FP-CIT Study Group. *Mov Disord.* 2000;15:503–510.
20. Chouker M, Tatsch K, Linke R, Pogarell O, Hahn K, Schwarz J. Striatal dopamine transporter binding in early to moderately advanced Parkinson's disease: monitoring of disease progression over 2 years. *Nucl Med Commun.* 2001;22:721–725.
21. Staffen W, Mair A, Unterrainer J, Trinka E, Ladurner G. Measuring the progression of idiopathic Parkinson's disease with [^{123}I] beta-CIT SPECT. *J Neural Transm.* 2000;107:543–552.
22. Pirker W, Djamshidian S, Asenbaum S, et al. Progression of dopaminergic degeneration in Parkinson's disease and atypical parkinsonism: a longitudinal beta-CIT SPECT study. *Mov Disord.* 2002;17:45–53.
23. Linke R, Gostomzyk J, Hahn K, Tatsch K. [^{123}I]IPT binding to the presynaptic dopamine transporter: variation of intra- and interobserver data evaluation in parkinsonian patients and controls. *Eur J Nucl Med.* 2000;27:1809–1812.
24. Studholme C, Hill DL, Hawkes DJ. Automated three-dimensional registration of magnetic resonance and positron emission tomography brain images by multiresolution optimization of voxel similarity measures. *Med Phys.* 1997;24:25–35.
25. Sychra JJ, Pavel DG, Chen Y, Jani A. The accuracy of SPECT brain activation images: propagation of registration errors. *Med Phys.* 1994;21:1927–1932.
26. Slomka PJ, Radau P, Hurwitz GA, Dey D. Automated three-dimensional quantification of myocardial perfusion and brain SPECT. *Comput Med Imaging Graph.* 2001;25:153–164.
27. Van Laere K, Koole M, D'Asseler Y, et al. Automated stereotactic standardization of brain SPECT receptor data using single-photon transmission images. *J Nucl Med.* 2001;42:361–375.

28. Hall H, Halldin C, Guilloteau D, et al. Visualization of the dopamine transporter in the human brain postmortem with the new selective ligand [^{125}I]PE2I. *Neuroimage.* 1999;9:108–116.
29. Tissingh G, Booij J, Bergmans P, et al. Iodine-123-n-omega-fluoropropyl-2beta-carbomethoxy-3beta-(4-iodophenyl)tropane SPECT in healthy controls and early-stage, drug-naive Parkinson's disease. *J Nucl Med.* 1998;39:1143–1148.
30. Booij J, Habraken JB, Bergmans P, et al. Imaging of dopamine transporters with iodine-123-FP-CIT SPECT in healthy controls and patients with Parkinson's disease. *J Nucl Med.* 1998;39:1879–1884.
31. Hwang WJ, Yao WJ, Wey SP, Ting G. Reproducibility of ^{99m}Tc-TRODAT-1 SPECT measurement of dopamine transporters in Parkinson's disease. *J Nucl Med.* 2004;45:207–213.
32. Seibyl JP, Laruelle M, van Dyck CH, et al. Reproducibility of iodine-123-beta-CIT SPECT brain measurement of dopamine transporters. *J Nucl Med.* 1996;37:222–228.
33. Tsuchida T, Ballinger JR, Vines D, et al. Reproducibility of dopamine transporter density measured with ^{123}I-FPCIT SPECT in normal control and Parkinson's disease patients. *Ann Nucl Med.* 2004;18:609–616.
34. Hughes AJ, Daniel SE, Ben-Shlomo Y, Lees AJ. The accuracy of diagnosis of parkinsonian syndromes in a specialist movement disorder service. *Brain.* 2002;125:861–870.
35. Hughes AJ, Daniel SE, Kilford L, Lees AJ. Accuracy of clinical diagnosis of idiopathic Parkinson's disease: a clinico-pathological study of 100 cases. *J Neurol Neurosurg Psychiatry.* 1992;55:181–184.
36. Schrag A, Ben-Shlomo Y, Quinn N. How valid is the clinical diagnosis of Parkinson's disease in the community? *J Neurol Neurosurg Psychiatry.* 2002;73:529–534.
37. Volkow ND, Fowler JS, Wang GJ, et al. Decreased dopamine transporters with age in health human subjects. *Ann Neurol.* 1994;36:237–239.
38. De Keyser J, Ebinger G, Vauquelin G. Age-related changes in the human nigrostriatal dopaminergic system. *Ann Neurol.* 1990;27:157–161.
39. Meyer PT, Sattler B, Lincke T, Seese A, Sabri O. Investigating dopaminergic neurotransmission with ^{123}I-FP-CIT SPECT: comparability of modern SPECT systems. *J Nucl Med.* 2003;44:839–845.
40. Hamann CS, Koch W, Radau PE, Tatsch K. Automated evaluation of dopamine D2 receptor SPECT studies: benefit in clinical routine [abstract]? *J Nucl Med.* 2003;44(suppl):261P–262P.

JNM The Journal of NUCLEAR MEDICINE

Clinical Testing of an Optimized Software Solution for an Automated, Observer-Independent Evaluation of Dopamine Transporter SPECT Studies

Walter Koch, Perry E. Radau, Christine Hamann and Klaus Tatsch

J Nucl Med. 2005;46:1109-1118.

The Journal of Nuclear Medicine is published monthly.
SNMMI | Society of Nuclear Medicine and Molecular Imaging
1850 Samuel Morse Drive, Reston, VA 20190.
(Print ISSN: 0161-5505, Online ISSN: 2159-662X)

SNMMI SOCIETY OF NUCLEAR MEDICINE AND MOLECULAR IMAGING